ASCE

Innovative Accelerated Curing of Cement Pastes Using Pulsed Electric Fields: Effect of Electric Field Intensities and Water Content on Hydration Kinetics and Compressive Strength

Chatchawan Kantala[1]; Natt Makul, M.ASCE[2]; and Phadungsak Rattanadecho[3]

Abstract: Conventional thermal curing techniques may reduce curing periods but frequently compromise long-term efficacy through microcracking and delayed ettringite proliferation. Pulsed electric field (PEF) processing offers an alternative methodology to expedite the hydration process without the drawbacks of high-temperature curing. In this investigation, cement pastes were formulated with varying water–cement (w/c) ratios (0.20–0.65) and subjected to different electric field intensities ranging from 0.5 to 1.5 kV/cm for durations of up to 50 min. Immediately after PEF treatment, specimens were air-cured at the ambient temperature (25 ± 2°C) for 28 days. Thermal profiles were monitored throughout curing to assess the hydration rate, and 28 day compressive strength evaluations were conducted to quantify the mechanical performance. Supplementary microstructural analyses were executed via scanning electron microscopy (SEM) to identify potential morphological alterations in the cement matrix arising from PEF. The results indicate that moderate PEF intensities (0.5 kV/cm) with an optimal w/c ratio (0.40–0.45) significantly accelerated early-age hydration rates, reaching thermal peaks approximately 5–6 h prior to those observed for the control specimens (0.0 kV/cm). Under these conditions, increases of up to 20% in the maximum compressive strength (reaching ~41 MPa at 28 days) were documented compared to conventional curing. Conversely, high electric field intensities (≥1.0 kV/cm) caused excessive thermal escalation (up to ~89°C for a w/c of 0.20), which gave rise to localized microcracking and attenuated strength at later ages. SEM inspections corroborated these observations, indicating denser hydration products and diminished porosity under optimal PEF conditions, whereas higher field strengths increased the porosity and microfissuring. In essence, the use of PEF under meticulously controlled conditions of field intensity and water content represents an effective, energy-efficient technique for promoting cement hydration. By diminishing the curing period without jeopardizing the long-term characteristics, PEF-enabled curing offers a promising next-generation approach for high-performance cementitious materials. Further investigation is advocated to optimize the field parameters, characterize the long-term durability under realistic environmental conditions, and extend this technique to full-scale concrete constructs. **DOI: 10.1061/JMCEE7.MTENG-22129.**

Practical Applications: This research on PEF processing offers significant practical applications for enhancing cement hydration in construction. When used with an optimized w/c ratio and moderate electric field intensities of ~0.5 kV/cm, PEF can substantially accelerate early-age hydration, resulting in strength improvements of up to 20% compared to conventional curing methods. This technology allows for reduced curing times, which is particularly beneficial in projects where time efficiency is crucial, such as in rapid construction environments or during adverse weather conditions. Further, the findings suggest that PEF processing could be implemented in the production of high-performance cementitious materials to ensure that the desired mechanical properties are attained promptly. The denser hydration products and improved microstructure obtained under optimal PEF conditions may lead to enhanced durability in concrete applications, making this process suitable for infrastructure that will be faced with harsh environmental conditions. As the construction industry increasingly embraces sustainable practices, PEF technology stands out as an energy-efficient solution that mitigates the long-term degradation issues associated with traditional thermal curing, positioning it as a promising method for advancing modern concrete technologies. Further exploration of this methodology could pave the way for its integration into large-scale concrete production.

Author keywords: Pulsed electric field (PEF); Accelerated curing; Cement paste; Hydration kinetics; Microstructural development; Compressive strength.

Introduction

Pulsed electric field (PEF) processing has emerged as an up-and-coming alternative to the prevailing accelerated curing methodologies, which predominantly depend on elevated thermal conditions to create rapid strength enhancements in cementitious materials (Che et al. 2025; Nepomnyashchev and Titov 2023; Ma et al. 2023; Wang et al. 2023). Thermal-based methods, such as steam curing, are characterized by substantial energy consumption and may have considerable drawbacks. The elevated temperatures that accelerate the hydration process frequently result in microcracking, as the rapid transfer of heat engenders pronounced thermal gradients within the

[1]Research Unit of Applied Electric Field in Engineering, College of Integrated Science and Technology, Rajamangala Univ. of Technology Lanna, Chiang Mai 50220, Thailand. Email: chatchawan_kantala@yahoo.com

[2]Professor, Dept. of Civil Engineering Technology, Faculty of Industrial Technology, Phanakhon Rajabhat Univ., 9 Chaengwattana Rd., Bangkhen, Bangkok 10220, Thailand. Email: natt@pnru.ac.th

[3]Professor, Dept. of Mechanical Engineering, Faculty of Engineering, Thammasat Univ., Pathum Thani 12120, Thailand (corresponding author). Email: ratphadu@engr.tu.ac.th

Note. This manuscript was submitted on April 3, 2025; approved on October 29, 2025; published online on June 20, 2026. Discussion period open until November 20, 2026; separate discussions must be submitted for individual papers. This paper is part of the ***Journal of Materials in Civil Engineering***, © ASCE, ISSN 0899-1561.

concrete matrix. This thermal incongruity can undermine the interfacial transition zone between the cement paste and the aggregates, thereby adversely affecting the material's long-term mechanical properties and durability.

The propensity for high temperatures to instigate delayed ettringite formation (DEF) is of particular concern. This phenomenon arises when sulphates are liberated during hydration and recrystallize within cracks or voids under cooler ambient conditions. DEF is acknowledged as one of the principal contributors to premature degradation in concrete infrastructures, often culminating in expansion and cracking. Moreover, the apparatus requisite for steam curing, which includes pressurized chambers and specialized boiler systems, incurs substantial operational expenditure, rendering large-scale or on-site implementations logistically onerous and environmentally detrimental due to elevated carbon emissions. In recent years, various innovative concrete curing techniques have been investigated with a view to enhancing the performance and sustainability of construction materials. Cementitious systems have been proposed that are capable of storing electrical energy, introducing a new dimension in which structural elements can also function as energy sources. Low-temperature microwave curing of ultrahigh-performance concrete has been shown to accelerate early strength development and to generate unique crystalline structures that are not observed with conventional curing methods. In addition, microwave curing in concrete repair applications has demonstrated significant reductions in curing time and energy consumption, although careful temperature control is required to ensure long-term quality. Moreover, electrical curing has been found to produce finer pore structures and consume less energy compared to steam curing.

Collectively, these advancements reflect a growing trend in the development of concrete curing technologies that emphasize efficiency, rapid strength gain, and environmental sustainability in modern construction (Huang et al. 2025; Li et al. 2025; Mangat et al. 2021; Yang et al. 2021). In contrast, PEF curing utilizes rigorously controlled electric fields rather than high heat to enable the hydration process to take place more rapidly. This focused electrical stimulation can reduce construction timelines without inducing the thermal stress and microstructural damage commonly associated with steam-cured concrete. Empirical studies have indicated that direct electric curing (DEC), a variant of PEF, can give a one-day compressive strength that approaches 90% of the strength typically observed at 28 days (Nepomnyashchev and Titov 2023; Ma et al. 2023). Further, the application of electric fields enhances the microstructural integrity by diminishing porosity and refining pore connectivity, thereby contributing to a stronger bond within the cement paste (Nepomnyashchev and Titov 2023; Ma et al. 2021). This renders PEF curing particularly advantageous for infrastructure initiatives that require high early-age strength while concurrently mitigating the risks of long-term deterioration. In addition to these performance enhancements, PEF-based techniques are associated with significantly lower energy consumption (occasionally as minimal as 1.18% of the energy required for steam curing when supplemented with accelerators), thereby presenting a more sustainable and economically viable approach to producing durable, high-performance concrete (Ma et al. 2023). Despite the necessity for precise regulation of the electric field parameters to avoid microfissuring and other adverse effects, the available evidence indicates that PEF curing effectively addresses the fundamental limitations of traditional thermal treatments while offering novel avenues for sustainable and efficient concrete production.

PEF is also increasingly being used to augment or modify cementitious materials, for example in processes such as microbial inactivation and aggregate recycling. However, the introduction of electric fields can profoundly transform the chemical and physical properties of cement-based systems, potentially jeopardizing their long-term durability and structural integrity. The principal constraints emerge from accelerated calcium leaching, increased vulnerability to sulphate attack, and significant alterations in microstructure, each of which can undermine the compressive strength. One notable concern is calcium leaching, which is exacerbated by ion migration under electric fields and results in a marked deterioration of the microstructure over time (Huang et al. 2023a). This phenomenon elevates porosity, particularly at the cathode, and diminishes the compressive strength of the mortar. The application of electric fields also accelerates the diffusion of sulphate ions into the matrix, intensifying sulphate attacks and causing more severe degradation than under conventional curing conditions (Liu et al. 2024). These effects are further amplified by elevated water–cement ratios, which give rise to enhanced permeability and expedited damage. Moreover, water electrolysis can generate bubbles and localized thermal fluctuations, while high-voltage pulses may induce plasma channels and thermal expansion pressures that collectively compromise the material's pore structure (Li et al. 2023; Osuna et al. 2022).

From an engineering perspective, the fundamental mechanism of PEF processing resides in its ability to facilitate rapid ionic migration and electroosmotic flow. In cementitious substances, such electric field-induced phenomena not only expedite the dissolution of clinker components but also increase the subsequent precipitation of calcium silicate hydrates and other products that are essential for strength enhancement. Unlike thermal treatments, which commonly lead to the introduction or aggravation of microcracking and postponed ettringite formation, PEF exerts minimal direct thermal energy, consequently preserving the overall durability. The voltage magnitude and pulse characteristics (e.g., duration, frequency) must be meticulously optimized to prevent undesirable thermal spikes and localized field intensities. Notwithstanding these considerations, however, the potential for reduced energy consumption, accelerated curing, and enhanced performance has attracted burgeoning academic and industrial interest in PEF processing as a sustainable alternative to traditional methods of expediting reactions in cement-based composites.

Collectively, these processes emphasize the long-term durability challenges encountered by PEF-treated cementitious materials and underscore the necessity for protective strategies (Smith et al. 2009). For instance, the incorporation of supplementary cementitious materials such as fly ash can alleviate specific detrimental impacts, including calcium leaching and excessive strength reduction (Kuznetsova et al. 2011). Nonetheless, additional research is needed to optimize the material composition and processing parameters and to develop protective methodologies that diminish the risk of structural degradation. Such endeavors are essential to fully exploit the advantages of PEF in cement-based systems while preserving the mechanical integrity of the material and its extending service life.

Cement hydration is inherently slow and requires extended curing periods to attain the mechanical strength and durability necessary for most structural applications. Conventional accelerated curing methods, such as steam or elevated-temperature treatments, can accelerate the hydration process but often at the expense of long-term performance. These methods may induce microcracking, aggravate DEF, and increase the overall energy demand. Consequently, there is a clear need for new, efficient techniques that expedite cement hydration without causing detrimental side effects. PEF represents a promising alternative due to its nonthermal mode of action, which selectively enhances the hydration kinetics while preserving microstructural integrity. However, effectively implementing this emerging technology requires a deeper understanding of how water content interacts with PEF to influence hydration pathways and the final microstructure. Investigations of PEF-assisted

curing under varying water–cement ratios will have critical implications for the scientific community and the construction industry. Elucidation of the theoretical mechanisms by which electric fields affect ion transport and reaction rates can lead to broader insights into cement chemistry and crystallization processes. From the standpoint of applications, PEF-based curing could enable the rapid, energy-efficient, and ecofriendly production of high-strength cementitious materials if optimized effectively. This technology could ultimately reduce CO_2 emissions, construction timelines, and material costs, making it particularly relevant in large-scale infrastructure projects where sustainability, reliability, and expedited construction are paramount. Moreover, the enhanced microstructural development achieved though this approach could extend the lifespan of cement-based structures, thus giving longer service intervals and diminished resource consumption over a project's entire life-cycle.

Mechanism of Accelerated Curing by Pulsed Electric Fields

In addition to simply moving ions, PEF can also influence the microenvironment of hydration reactions. Short, high-intensity pulses introduce localized electrical currents that are capable of breaking down any transient passivating layers on the surfaces of partially hydrated cement grains (Susanto et al. 2015; Bredenkamp et al. 1993). The pulsed nature of the field reduces the risk of excessive Joule heating, a common challenge in direct current or continuous high-voltage methods, while still transiently raising the local temperatures sufficiently to speed up the chemical kinetics. Concurrently, electroosmotic flow can improve pore connectivity and fluid transport, further ensuring that water and dissolved ions reach unhydrated cement particles. Moreover, repetitive pulsing can help disrupt or destabilize clusters of unreacted grains, thereby increasing their surface area exposed to water. Taken together, these electrodriven effects significantly shorten induction periods, enhance the rate of hydration product formation, and ultimately yield a denser, more homogeneously hydrated cement paste in far less time than standard curing practices. We present two sets of equations, one of which characterizes the ionic translocation phenomenon in the presence of an applied electric field and the other clarifies the essential hydration reactions in cement, thus jointly contributing to the understanding of the mechanism by which PEF facilitates curing (Susanto et al. 2015; Yang et al. 2017; Gawel et al. 2022; Bredenkamp et al. 1993).

Nernst–Planck Equation for Ionic Transport

When an electric field E is applied to a cement paste, the flux J_i of each ionic species (e.g., Ca^{2+}, OH^-) within the pore solution can be described by the Nernst–Planck equation [Eq. (1)] (Huang et al. 2023b)

$$J_i = -D_i \nabla c_i + z_i F \mu_i c_i E \tag{1}$$

where D_i = the diffusion coefficient of Species i; c_i = the concentration of Species iii in the pore solution; z_i = the ionic charge (valence); F = the Faraday constant (approximately 96,485 $C \cdot mol^{-1}$); μ_i = the ionic mobility (related to how easily Species iii moves under an electric field); and E = the electric field vector. The first term on the right, $-D_i \nabla c_i$, therefore represents diffusion driven by concentration gradients, while the second term, $z_i F \mu_i c_i E$, represents migration due to the applied electric field. In PEF curing, the repeated short bursts of the electric field enhance ion transport in and around the hydrating cement grains, thus expediting the formation of hydration products.

Hydration Reactions in Cement

Under normal (nonelectric) conditions, tricalcium silicate (C_3S), dicalcium silicate (C_2S), tricalcium aluminate (C_3A), and tetracalcium aluminoferrite (C_4AF), one of the main clinker phases in composite cement, form hydrates as shown in Eqs. (2)–(5)

$$C_3S + (x+y)H_2O \rightarrow C_x\text{-}S_y\text{-}H_z + CH + \Delta H \text{ or } 2C_3S + 6H_2O \rightarrow C_3S_2H_3 + 3Ca(OH)_2 \tag{2}$$

$$2C_2S + 4H_2O \rightarrow C_3S_2H_3 + Ca(OH)_2 \tag{3}$$

$$3CaO \cdot Al_2O_3 + 6H_2O \rightarrow 3CaO \cdot Al_2O_3 \cdot 6H_2O \tag{4}$$

$$C_4AF + 10H_2O \rightarrow C_3AH_6 + C_3FH_6 \tag{5}$$

where C_3S = tricalcium silicate (often written as $3CaO \cdot SiO_2$); $C_x\text{-}S_y\text{-}H_z$ = calcium silicate hydrate, the primary binder phase responsible for strength; CH = calcium hydroxide ($Ca(OH)_2$); ΔH indicates the exothermic heat released; and x and y = stoichiometric coefficients representing water consumption and product formation. When PEF is applied, ionic species such as Ca^{2+} and OH^- move more efficiently though the pore solution (as described by the Nernst–Planck equation above), thereby accelerating the dissolution of cement grains and the subsequent precipitation of hydration products. This results in faster formation of C–S–H, which leads to improved early-age strength and a denser microstructure compared to conventional curing methods.

By incorporating these processes, the electric field element present in the Nernst–Planck equation significantly boosts ionic mobility, consequently reducing the induction phase of cement hydration and facilitating the rapid deposition of C–S–H and CH. This intensified ion transport also facilitates a more uniform and dense development of the hydration products, augmenting the packing density and decreasing the occurrence of substantial pores. Consequently, the swift generation of C–S–H engenders elevated early-age strength while potentially reducing the overall curing durations and sustaining (or even augmenting) long-term durability.

Materials and Methods

This study involves a systematic investigation of how varying the water content and PEF treatments influence the hydration and mechanical characteristics of cement pastes. Ten distinct cement–water ratios (w/c = 0.20, 0.25, 0.30, 0.35, 0.40, 0.45, 0.50, 0.55, 0.60, and 0.65, w/w) are used to capture the effect of water content on early-age and long-term performance. Each formulation is cured under two principal conditions: (1) conventional air curing (control); and (2) PEF-assisted curing at electric field intensities of 0.5, 1.0, and 1.5 kV/cm for a treatment time of 50 min. Specimens subsequently undergo a standardized 28-day air-curing regimen at 25 ± 2°C. By characterizing the physical and mechanical attributes, such as the compressive strength and microstructural characteristics, this research aims to elucidate the role of the water content and the electric field parameters in expediting cement hydration and enhancing the overall material performance, as shown in Fig. 1.

Materials

In this investigation, hydraulic cement (HC), type *GU*, for general construction adhering to ASTM C1157 (ASTM 2017), was used as the cementitious material. Scanning electron microscopy (SEM) images of HC particles (2,000×) and X-ray diffraction (XRD) results for HC quantity of compound name and chemical formula are shown in Figs. 2(a and b). The cement was procured from a regional

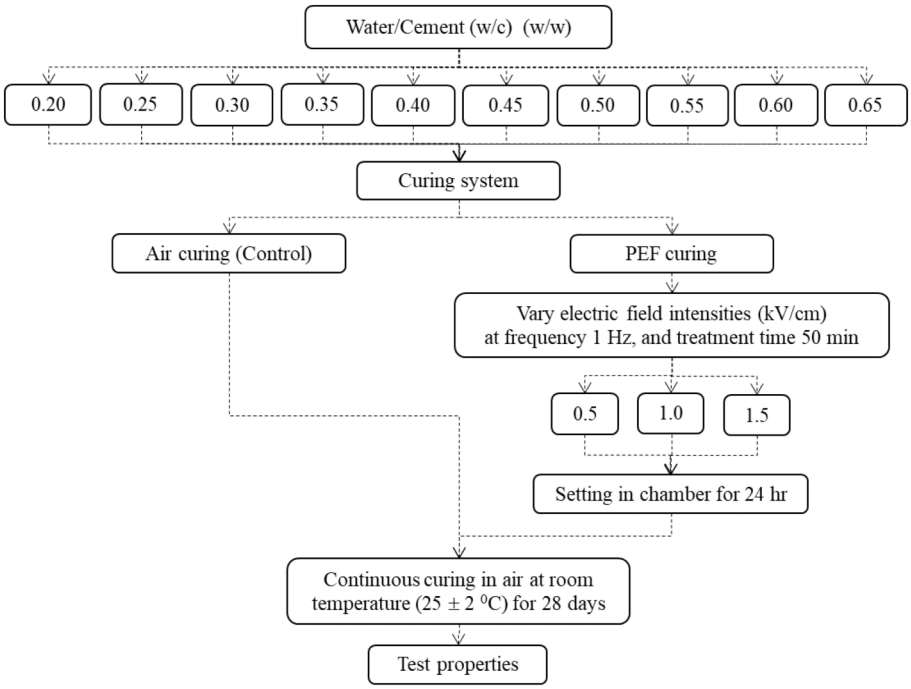

Fig. 1. Scope of the study.

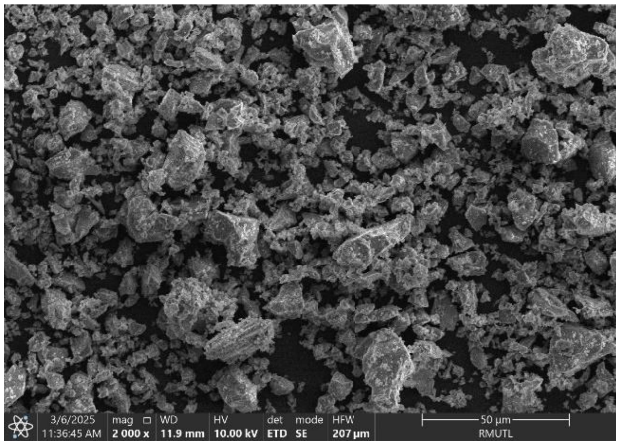

(a)

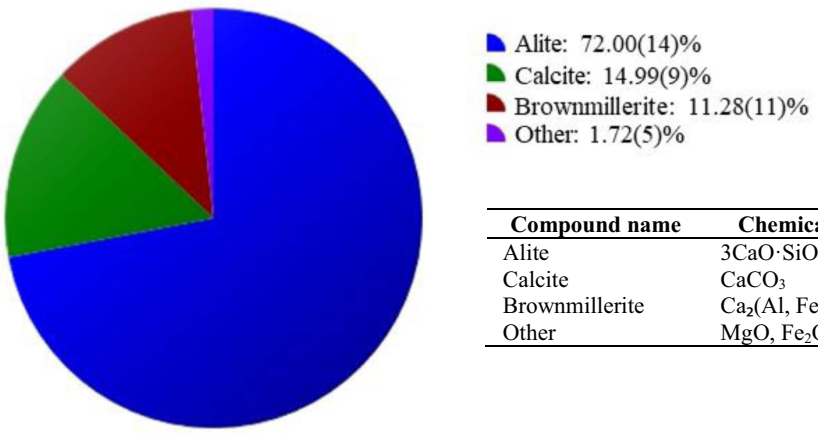

Compound name	Chemical formula	Quantity (%)
Alite	$3CaO{\cdot}SiO_2$	72.00
Calcite	$CaCO_3$	14.99
Brownmillerite	$Ca_2(Al, Fe)_2O_5$	11.28
Other	MgO, Fe_2O_3	1.75

(b)

Fig. 2. (a) SEM microscopic of HC particles (2,000×); and (b) XRD results of HC quantity of compound name and chemical formula.

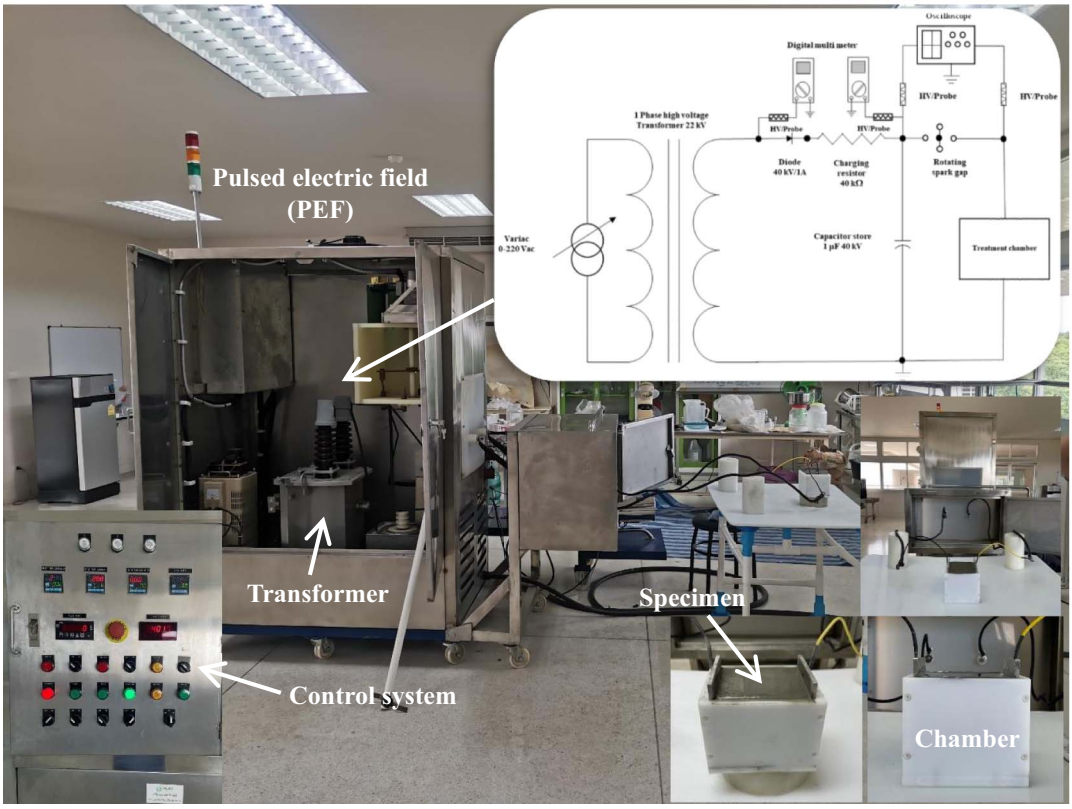

Fig. 3. PEF apparatus.

producer in Thailand to ensure conformity with pertinent quality assurance protocols. Further, purified, filtered water with a neutral pH was employed for amalgamation and curing, thereby preserving uniform hydration conditions throughout the experimental process.

PEF Processing

Fig. 3 depicts the PEF apparatus engineered for this investigation. The configuration consists of a single-phase high-voltage transformer rated at 22 kV, powered by a supply that is adjustable from 0 to 220 V AC. The transformer's secondary terminal is linked to a diode (40 kV/1 A) and a charging resistor, which collectively modulate the charging current of a 1 μF, 40 kV capacitor. Once the capacitor attains the requisite charge level, a rotating spark gap discharges the accumulated energy into the treatment chamber. High-voltage probes (HV/probe) are situated at strategic positions to quantify voltage waveforms, and the signals are recorded by a digital multimeter and an oscilloscope for contemporaneous monitoring and diagnostics. In execution, the rapid discharge of the high-voltage capacitor though the spark gap engenders short-duration, high-voltage pulses that are transmitted into the cementitious sample within the treatment chamber. By modulating the applied voltage (0–220 V_{AC}) and adjusting the spark gap, the magnitude (kV/cm) and frequency of pulsed discharges can be finely adjusted. This degree of regulation is imperative in order to ensure that the PEF treatment expedites hydration without engendering adverse thermal spikes or microstructural impairment. The schematic representation in Fig. 3 shows each principal component and its function in pulsed generation, measurement, and sample treatment, thereby providing a comprehensive overview of the PEF operation employed in this research.

High-voltage probes (HV/probe) are situated anterior and posterior to the spark gap to enable real-time observation of voltage waveforms, with measurements made via a digital multimeter and oscilloscope. The angular velocity of the rotating spark gap can be modified to adjust the pulse repetition frequency, while the voltage across the capacitor is controlled by the varies on the primary side. These mechanisms facilitate careful calibration of the pulse amplitude (0.5–1.5 kV/cm, as aimed for in this investigation), frequency, and treatment duration (10–50 min) to align with the specific experimental aims. The dimensions of the treatment chamber (for instance, 300 × 300 × 300 mm, or sized in accordance with the desired specimen morphology) are engineered to accommodate standard cement cubes (100 × 100 × 100 mm) or other test configurations. Within this enclosure, the electric pulses traverse uniformly though the specimen, augmenting the hydration kinetics without producing the substantial thermal gradients that frequently arise in continuous high-voltage or steam-curing systems. By systematically manipulating the voltage levels, pulse durations, and water–cement ratios, researchers can isolate the optimal PEF conditions for expediting early-age strength development and enhancing microstructural evolution in cement-based materials.

Mixing and Specimen Preparation

All mixing procedures were carried out for 10 min following the protocol illustrated in Fig. 1. The HC (of type *GU*) was combined with water at various w/c ratios of 020–0.65 using a mechanical mixer. The fresh mixed paste was then cast into a custom-designed chamber mold to produce 100 × 100 × 100 mm specimens in accordance with BS 1881: Part 3 (BSI 1983), as shown in Fig. 3. These samples were subsequently subjected to PEF curing followed by air curing.

Cement paste specimens were prepared by thoroughly blending HC with water in a mechanical mixer at the specified ratios. Specimens measuring 100 × 100 × 100 mm were then cast and allowed to set at room temperature (25 ± 2°C). Two curing methods were employed: air curing (control) and PEF curing with electric field intensities of 0.5–1.5 kV/cm at a frequency of 1 Hz, with the number

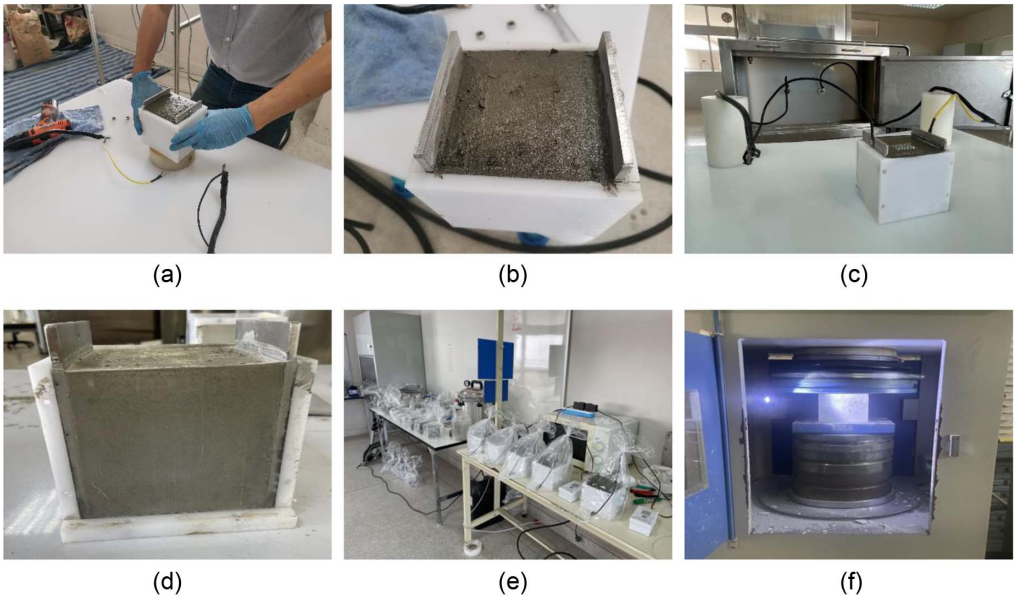

Fig. 4. Specimen preparation and testing: (a) assemblage of specimen in mold; (b) specimen before PEF curing; (c) specimen connected to two electrodes, positive (+) and negative (−); (d) specimen after PEF curing; (e) specimens to be cured until testing time; and (f) specimens under compressive test.

of pulses varying in the range 0, 10, 20, 30, 40, and 50 min. For PEF curing, as shown in Figs. 4(a and b), after mixing, the cement paste was poured into the mold in three layers, with each layer being uniformly tamped or vibrated to remove entrapped air. Once the final layer had been placed, the surface was leveled off, and the specimens were covered to maintain a consistent humidity and temperature. The molded specimens were then left undisturbed for 24 h at room temperature (25 ± 2°C) before the subsequent curing or demoulding procedures. For PEF treatment, each molded specimen was carefully positioned between two electrodes, to ensure secure and uniform contact with the electrode surfaces. This arrangement enabled the PEF to be applied effectively though the cement paste, thereby accelerating the hydration process while preserving uniform treatment conditions, as shown Fig. 4(c). After the PEF curing process, each specimen was removed from the curing chamber and transferred to a controlled environment. From this point onward, specimens were cured under standard conditions until the designated testing age of 28 days [Figs. 4(d–f)].

Results and Discussion

Temperature Rise during Curing with PEF and Continuous Curing with Air

Fig. 5 shows the correlation between the fluctuating electric field intensities at 0 (control), 0.5, 1.0, and 1.5 kV/cm and the hardening rate of the cement pastes. As the field strength escalates, the hardening rate increases correspondingly. Further, the w/c was modified within the range of 0.20 to 0.65. In the absence of an electric field (0.0 kV/cm) and a minimal w/c of 0.25, the specimen attained its peak hardening temperature of 61.0°C at 4.5 h, whereas at w/c = 0.65, the base peak of 45.6°C was observed at 8.7 h. When specimens were exposed to PEF for 50 min, followed by air curing at 25 ± 2°C for 28 days, the 0.5 kV/cm condition exhibited a comparable temperature and duration to the control. However, increasing the field to 1.0 kV/cm resulted in a maximum temperature of 73.8°C at 2.7 h (w/c = 0.25), with the lowest peak of 52.7°C occurring at 5.0 h (w/c = 0.65). At 1.5 kV/cm, the temperature intensified to 89.2°C at 1.8 h (w/c = 0.20) and subsequently diminished to 69.0°C at 2.4 h for w/c = 0.60. Thereafter, all specimens (PEF-treated and untreated) were enveloped in plastic and air-cured for an additional 24 h at the ambient temperature and then preserved until 28 days for an assessment of the mechanical properties. Notably, after attaining each maximum hardening temperature, the temperature declined due to waning hydration reactions (Makul and Sua-iam 2024; Sánchez et al. 2024).

Fig. 5 illustrates the different temperature profiles observed for cement pastes subjected to PEF curing compared to those under conventional control conditions (0 kV/cm). Under control curing, the gradual exothermic reaction of tricalcium silicate (C_3S) and other clinker phases causes the temperature to reach a modest peak, usually between 50°C and 60°C, over several hours. In contrast, the application of PEF at intensities of 0.5, 1.0, or 1.5 kV/cm triggers a steeper rise in temperature within a considerably shorter timeframe, often culminating in peak values 10°C–30°C above the control. As depicted in Fig. 5(b), a moderate electric field of 0.5 kV/cm yields a rise to approximately 55°C–60°C within roughly 5 h, reflecting accelerated ion transport and hydration reactions. At 1.0 kV/cm, as shown in Fig. 5(c), the peak temperature becomes closer to 70°C–75°C in under 3 h. Meanwhile, the highest applied field of 1.5 kV/cm [Fig. 5(d)] drives the system to a temperature of around 85°C–90°C in as little as 2 h, demonstrating the potency of pulsed fields in expediting exothermic cement reactions.

To understand this rapid temperature escalation, the Nernst–Planck equation for ionic transport is helpful. In conventional diffusion-driven hydration, species such as Ca^{2+} and OH^- move though the pore solution, chiefly in response to concentration gradients. However, the electromigration term in the Nernst–Planck equation, $J_i = -D_i\nabla c_i + z_i F\mu_i c_i E$, becomes dominant under an external electric field, particularly under the short, high-voltage pulses characteristic of PEF (Huang et al. 2023c). The factor $J_i z_i F\mu_i c_i E$ greatly enhances ion flux, thereby increasing the availability of reactants at the surfaces of unhydrated cement grains. This prompts a quicker onset of the exothermic hydration reactions that generate calcium silicate hydrate (C–S–H), calcium hydroxide (CH), and other products (Rolle et al. 2018; Horne 1983). The faster and more localized these reactions become, the more abruptly heat is released. Indeed, the relationship between electric field intensities and temperature peaks is almost proportional when other variables, such as

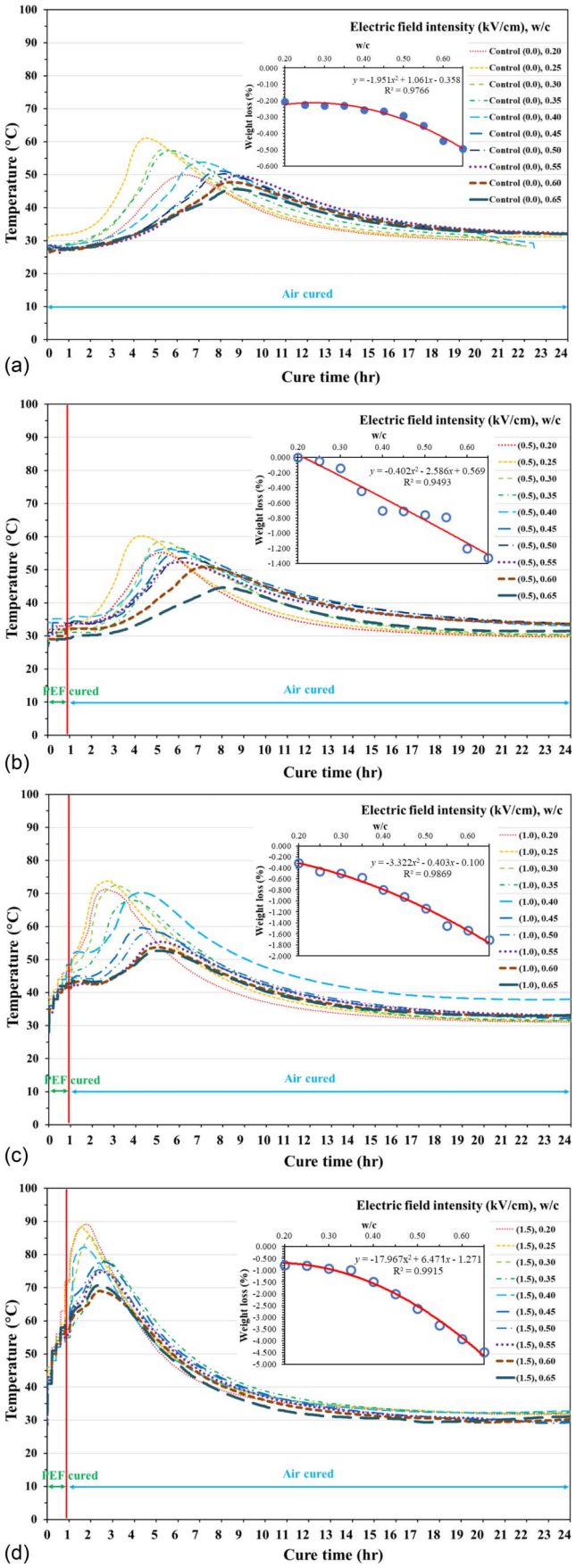

Fig. 5. Temperature and curing times for air-curing: (a) control (0.0 kV/cm) and accelerated curing with PEF for 0–50 min and continued incubation for 24 h at electric field intensities 0.5–1.5 kV/cm; (b) PEF at 0.5 kV/cm; (c) PEF at 1.0 kV/cm; and (d) PEF at 1.5 kV/cm.

the w/c ratio, remain constant. In practice, lower w/c ratios (e.g., 0.20–0.30) give a denser matrix with fewer water-filled pores and thus less ability to dissipate heat; consequently, temperature spikes of up to 85°C–90°C are observed at 1.5 kV/cm. Although such high temperatures can promote remarkably swift strength development, they also create a risk of microcracking from thermal gradients if the interior and exterior of the specimen cool at different rates once PEF treatment ceases.

From the standpoint of hydration chemistry, the exothermic reactions at play, particularly those involving C_3S and dicalcium silicate (C_2S), are heavily influenced by the local concentration of ionic species. The application of PEF mobilizes these ions more efficiently and produces intermittent bursts of energy that reduce the induction period, effectively shifting a significant portion of the hydration exotherm into an earlier time window. Without an electric field, the induction phase might last several hours, whereas with PEF, the same phase may be completed in under an hour, hastening the point at which C–S–H gel nuclei proliferate (He et al. 2018; Hao et al. 2022; Engel'sht and Muratalieva 2013; Qi et al. 2021). The localized increase in temperature resulting from these newly formed hydrates further boosts the chemical kinetics, creating a feedback loop of early-age heat release. Hence, Figs. 5(b–d) can be viewed as a visual representation of this synergy: fields of 0.5, 1.0, and 1.5 kV/cm progressively ramp up ion transport and, by extension, accelerate the hydration exotherm.

It can be observed that, once the PEF treatment concludes, specimens are typically transitioned to an air-curing environment at 25 ± 2°C. This phase stabilizes the cement matrix after the intense heat buildup shown in Figs. 5(a–d). In practical terms, the subsequent cooling behavior is intimately linked to the high temperature reached during PEF curing and the w/c ratio, which dictates the thermal conductivity and specific heat capacity of the paste. If the peak temperature surpasses 80°C–85°C, which is often the case under 1.5 kV/cm, then the interior region may remain hotter than the surface for an extended period, creating a potential for thermal stress as the surface cools more rapidly. This mismatch can spawn microcracks or interfacial defects, especially at lower w/c ratios where the microstructure is already dense and less forgiving of abrupt volumetric changes. Nevertheless, many experiments demonstrate that if the field intensity is moderate (around 0.5 to 1.0 kV/cm) and the w/c ratio is kept in the range 0.40–0.50, the temperature peaks at around 60°C–75°C. While this is notably higher than for control curing, it remains below the critical thresholds associated with widespread thermal damage.

From a mechanistic perspective, the final shape of the temperature-time curve represents a balance between ongoing exothermic hydration, which is driven by the chemical transformations of C_3S and the other clinker phases and heat dissipation into the ambient environment. The simplified hydration reactions show the following. The release of ΔH slows after the first few hours, once the availability of fresh cement grains and unreacted water diminishes. Consequently, although PEF compresses the induction period and accelerates early C–S–H formation, the rate of heat release tapers as the sample ages. If air curing proceeds uniformly, the specimen gradually equilibrates, allowing hydration to continue below damaging temperatures. This gentle cooling phase also helps avoid the rapid contraction that could exacerbate cracking, as mild temperature differences are far less likely to induce significant tensile stresses. Moreover, the Nernst–Planck-driven ionic flux that takes place during pulsing may persist at a lower intensity when the electric field is removed, an effect that is primarily governed by diffusion and any mild electrostatic residuals within the matrix. By the time the system enters the pure air-curing mode, much of the microstructural densification, which is associated with robust C–S–H formation, will

Table 1. Temperature tests during accelerated curing at various electric field intensities and w/c ratios

	Control (air-curing)		0.5 kV/cm		1.0 kV/cm		1.5 kV/cm	
w/c	Temp. max (°C)	Time (h)	Temp. max (°C)	Time (h)	Temp. max (°C)	Time (h)	Temp. max (°C)	Time (h)
0.20	50.8	6.2	55.2	5.2	71.4	2.5	89.2	1.8
0.25	61.0	4.5	60.3	4.3	73.8	2.7	88.6	1.7
0.30	57.6	5.2	58.7	5.2	72.4	3.1	85.9	2.0
0.35	57.2	5.6	56.8	5.9	68.0	3.8	78.4	2.7
0.40	53.7	7.6	56.3	5.4	70.3	4.2	82.2	1.6
0.45	51.2	7.8	55.6	6.2	59.6	4.3	77.8	2.5
0.50	50.2	8.1	53.6	6.3	58.4	4.7	75.4	2.4
0.55	49.7	8.8	52.4	6.0	55.4	5.2	74.8	2.6
0.60	47.7	8.5	50.9	7.2	53.8	5.1	69.0	2.4
0.65	45.6	8.7	44.6	8.1	52.7	5.0	70.8	2.4

have already been established. Upon microscopic inspection, researchers often observe that these specimens possess higher early strengths (compared to non-PEF or control samples) and a more homogeneous microstructure. Pore distribution tends to be more uniform, and the interfacial transition zones are less porous, yielding improved mechanical properties over extended curing times. Thus, the temperature spike indicated in Figs. 5(b–d) is not merely a byproduct of PEF curing but an integral driver that reshapes the hydration profile. The temperature rise illustrated in Figs. 5(a–d) therefore highlights the powerful impact of PEF on cement paste hydration temperatures and the essential interplay of the Nernst–Planck equation with exothermic cement reactions. Although the higher temperature peaks give earlier strength gains and microstructural refinement, they must be judiciously managed to circumvent thermal damage. By coupling optimized PEF parameters, such as field intensity, pulse duration, and frequency, with balanced w/c ratios and a proper cooling regimen, the advantages of rapid hydration can be harnessed while preserving long-term durability. This synergy ultimately positions PEF curing as a compelling alternative to conventional high-temperature methods, as it offers a means of achieving fast, energy-efficient cement curing without the inherent drawbacks of steam curing or autoclaving [Lee et al. 2023; Wu 2023; E. Demir et al., "Method involving PEF treatment and drying," US Patent No. 20,200,281,219A1 (2017); Schottroff et al. 2020].

Table 1 illustrates how the PEF intensity and w/c ratios together shape the maximum temperature reached during accelerated curing (and the time taken to achieve that peak) for cement paste specimens. It can be observed that higher electric field intensities are correlated with faster and higher temperature rises, an outcome consistent with PEF's capacity to enhance ionic movement and expedite the exothermic hydration reactions.

We also note the effect of varying the w/c ratio from 0.20 to 0.65: smaller w/c values (i.e., more cement relative to water) show more pronounced heating under PEF, whereas higher w/c ratios moderate these thermal escalations. A clear pattern emerges for the 0 kV/cm (control) column. As the water content increases, the maximum temperature and time taken to reach it generally declined or lengthened, respectively. For example, at 0.25, control samples reached a peak of 61.0°C in 4.5 h, whereas a value of 0.65 gave a substantially lower peak of 45.6°C but required 8.7 h, almost double the time. This finding emphasizes the well-established notion that a denser matrix (i.e., lower w/c) produces more rapid and higher thermal buildup, because the hydration process is less diluted by excessive water and the generated heat has fewer pathways for dissipation (Mengistu et al. 2017; Lyutikova et al. 2020).

Under 0.5 kV/cm, the test results show a small increase in peak temperature compared to the control and a shorter time to reach that peak in some cases. Notably, at w/c = 0.25, the maximum temperature reaches 60.3°C in 4.3 h, similarly to the results for the control of 61.0°C at 4.5 h. This suggests that a level of 0.5 kV/cm does not drastically alter the temperature profile for mixtures near the "sweet spot" of hydration (i.e., neither too wet nor too dry). However, for the other w/c values of 0.20, 0.30, etc., there remains a consistent pattern of slightly higher final temperatures than for the control, often accompanied by shorter times to achieve those peaks. At a w/c of 0.20, for instance, raising the field from zero to 0.5 kV/cm raises the temperature from 50.8°C to 55.2°C and shortens the time from 6.2 to 5.2 h. Although these changes are moderate, they signal that even a relatively low electric field can measurably accelerate hydration-induced heat release.

A significant change appears at 1.0 kV/cm, where almost every mixture undergoes a considerable increase in peak temperature, often 15°C–20°C above the control, and a corresponding reduction in the peak time by about half. A case in point is w/c = 0.20, where the temperature rises from 50.8°C (control) to 71.4°C, while the time is reduced from 6.2 to 2.5 h. Meanwhile, at a w/c of 0.65, the peak temperature of 52.7°C is reached in only 5.0 h, as opposed to 45.6°C at 8.7 h for the control. These observations corroborate that a mid-range electric field (particularly 1.0 kV/cm) profoundly expedites the hydration exotherm for various values of the water content. The effect is most dramatic in the low w/c domain, where the matrix is dense and less heat is lost to the surroundings.

When the intensity is increased to 1.5 kV/cm, the data highlight the potential risks of a thermal climb that is too rapid. Under these conditions, samples at a lower w/c are raised to extremely high temperatures, peaking at 89.2°C for a w/c of 0.20, within just 1.8 h. Even mixtures in the upper water-content region undergo significant thermal surges: for instance, a w/c of 0.65 gives a value of 70.8°C in 2.4 h, a temperature and rate of rise rarely seen under any regular curing regime. Such swift and intense heating could translate to microstructural distress, including microcracks and uneven pore distribution, particularly in the relatively rigid, low-porosity pastes. The final columns of Table 1 consistently show higher maximum temperatures and significantly shortened times to peak for 1.5 kV/cm, underscoring how aggressively the electric field drives ion transport and thus the exothermic reactions responsible for the temperature upswing.

Another instructive aspect is the way in which the temperature-time profile for each mixture shifts relative to the baseline hydration. For the control samples, the maximum temperatures generally occur in the range 4.5 to 8.7 h across all w/c values, reflecting the natural cement hydration kinetics. In contrast, the application of 1.5 kV/cm frequently cuts that peak time by more than half (sometimes to less than 2 h), thereby compressing the thermal curve into a smaller window. This compression implies a high degree of acceleration for the early hydration phases, which is beneficial in terms of fast strength gain but may be deleterious if stress differentials, vapor

formation, or local hot spots are not managed. After these maximum temperatures have been reached, further data (discussed in the text, though not shown in the table) indicate that the temperature levels are gradually reduced as hydration decelerates, especially once the specimens are transitioned to ambient air curing.

For practical applications, the patterns revealed here confirm that the interplay between electric field intensity and water content is fundamental in terms of controlling the extent and the velocity of thermal buildup. A moderate approach, such as 0.5 kV/cm combined with a balanced w/c ratio (e.g., 0.40 to 0.45), tends to yield temperature peaks at around 55°C within a reasonable time frame (4–6 h), which can safely accelerate curing without overshooting into dangerous thermal zones. Conversely, extreme values of 1.5 kV/cm and w/c of 0.20 may push the hydration reactions to extreme rates, potentially causing early-age cracking if cooling or subsequent curing practices are not carefully regulated. Consequently, the results presented here serve as a quantitative guide for identifying the operational range over which PEF-based curing can optimize early strength development while minimizing thermal damage. By highlighting how incremental increases in field strength amplify the temperature peak and reduce the time to reach that peak for a given w/c, these results lay a solid empirical foundation for calibrating PEF conditions to achieve efficient, robust curing regimens.

The rapid temperature rises induced by PEF accelerate evaporation drive earlier and more rapid water loss, especially in mixes with moderate or low w/c ratios. Although higher w/c systems absorb heat more effectively, they still show a steeper evaporation slope (calculated as the rate of sample weight loss over time) than air-cured controls. At 1.0 kV/cm, peak temperatures of over 70°C amplify the evaporation rates within 3 h, risking insufficient residual water for complete hydration. In low w/c mixtures, localized interior temperatures can climb above 75°C, hastening water outflow. At 1.5 kV/cm, temperatures may exceed 85°C in under 2 h, causing extreme water loss and fostering local dryness, "shell" formation, and potential microcracks or voids. Ultimately, higher, earlier temperature peaks are directly correlated with intensified evaporation. Careful moderation of the field intensity and w/c ratio prevents excessive dehydration while still giving the benefits of rapid hydration.

Compressive Strengths of the Pastes Cured by PEF Compared to Air Curing

Fig. 6 presents the compressive strengths of cement paste specimens after a 50 min PEF treatment followed by an additional 28 day air-curing period. The horizontal axis shows the different w/c ratios, ranging from 0.20 to 0.65, while the vertical axis reflects the compressive strength achieved at 28 days. The data reveal strong interplay between water content and electric field intensity, with the control samples (0 kV/cm) offering a baseline for performance comparisons. Notably, for the control samples at a w/c of 0.20, the compressive strength is around 23.3 MPa, which increases steadily to approximately 36.0 MPa at a slightly higher w/c range (roughly 0.30–0.50) and then tapers off to 19.3 MPa at w/c of 0.65. This reduction in strength at a high water content reflects the conventional understanding that excess water leads to larger pores and lower density, thereby diminishing the compressive strength. In contrast, specimens exposed to PEF show a more complex pattern: the responses of the mixtures differ significantly at a field strength of 0.5–1.5 kV/cm, thus underlining the importance of carefully balancing the electric field intensity against water content (Zhang et al. 2024).

At a w/c of 0.20, the compressive strength under PEF exceeds that of the corresponding control sample, especially at field intensities of up to 0.5 kV/cm. This improvement suggests that PEF can accelerate early hydration and refine microstructure in dense, low-water mixes, leading to higher strength after 28 days of air curing. However, this trend changes when the w/c ratio is between 0.25 and 0.40, as in this range, many PEF-cured specimens exhibit a lower compressive strength than the control. The most likely explanation for this is that a moderate water content, combined with certain PEF conditions, can either generate localized overheating or disrupt the formation of hydration products, possibly fostering microcracks or a nonuniform C–S–H network. Once the w/c ratio reaches 0.45, however, a value of 0.5 kV/cm again appears to be beneficial, yielding a compressive strength peak of approximately 41.0 MPa. For values of the w/c ratio between 0.45 and 0.60, the best results emerge at 0.5 kV/cm, indicating a sweet spot where the electric field is sufficiently strong to accelerate hydration without causing deleterious microstructural disturbances. In contrast, higher electric field intensities of 1.0 kV/cm and above appear to reintroduce the risk of microcracks, which can be seen upon visual inspection or SEM imaging. Figs. 7(a and b) show microstructure images (2,000×) of the C–S–H network and pore percentages: Fig. 7(a) shows the control samples at 30.247%, Fig. 7(b) shows the results for 0.5 kV/cm of 28.613%, Fig. 7(c) shows the results for 1.0 kV/cm of 31.092%, and Fig. 7(d) shows the results for 1.5 kV/cm of 41.134%. In these cases, once microcracks form in the early curing stages, they can propagate or remain as flaws in the matrix, thereby undermining late-age strength development.

We also note that excessive electric field intensity can create larger porosity within the paste matrix, especially at very low w/c ratios. Fig. 7 shows cracks and gaps in the specimens at 1.0 and 1.5 kV/cm, thereby reinforcing the conclusion that moderate PEF levels of around 0.5 kV/cm are optimal in many scenarios. The synergy of mild electric field acceleration (boosting early hydration) and balanced water content (ensuring adequate workability and heat dissipation) yields the densest possible arrangement of C–S–H. By extension, it avoids the "shell effect," wherein rapidly formed hydration products enclose unhydrated cement grains, making the interior prone to cracking. From these results, 0.5 kV/cm emerges as the condition that maximizes the compressive strength while minimizing the thermally driven or stress-induced flaws that may appear with greater electric field intensities.

To understand the underlying mechanisms responsible for the variations in compressive strength, we can link these findings to the electrochemical and thermal processes described earlier. During PEF curing, short, high-voltage pulses accelerate the movement of ionic species, particularly Ca^{2+} and OH^{-}, through the pore fluid of the cement. Although this phenomenon can greatly expedite initial hydration and strengthen the structure, the process is sensitive to local heat buildup and water availability. When w/c is especially low (e.g., 0.20), the paste has a limited content of free water, so if the electric field intensity is too high ($\geq$ 1.0 kV/cm), rapid hydration may produce localized hot spots and internal stresses that cancel out any gain in reaction speed. On the other hand, at a modest field of 0.5 kV/cm, the hydration front is accelerated just enough to form a robust network of C–S–H before destructive thermal gradients or microcracking can set in.

In the midrange w/c levels of 0.25 to 0.40, one might expect a more moderate thermal response during PEF, but these samples do not show continual improvement in terms of compressive strength compared to the control. This slight underperformance may stem from a moderate or slightly lower water content combined with an electric field, which is prone to forming a superficial layer of dense hydration products that envelop the unhydrated cement. This "shell effect" can impede later hydration and lead to a less homogeneous microstructure overall. In addition, water electrolysis, which is particularly relevant at higher voltages, can produce microbubbles,

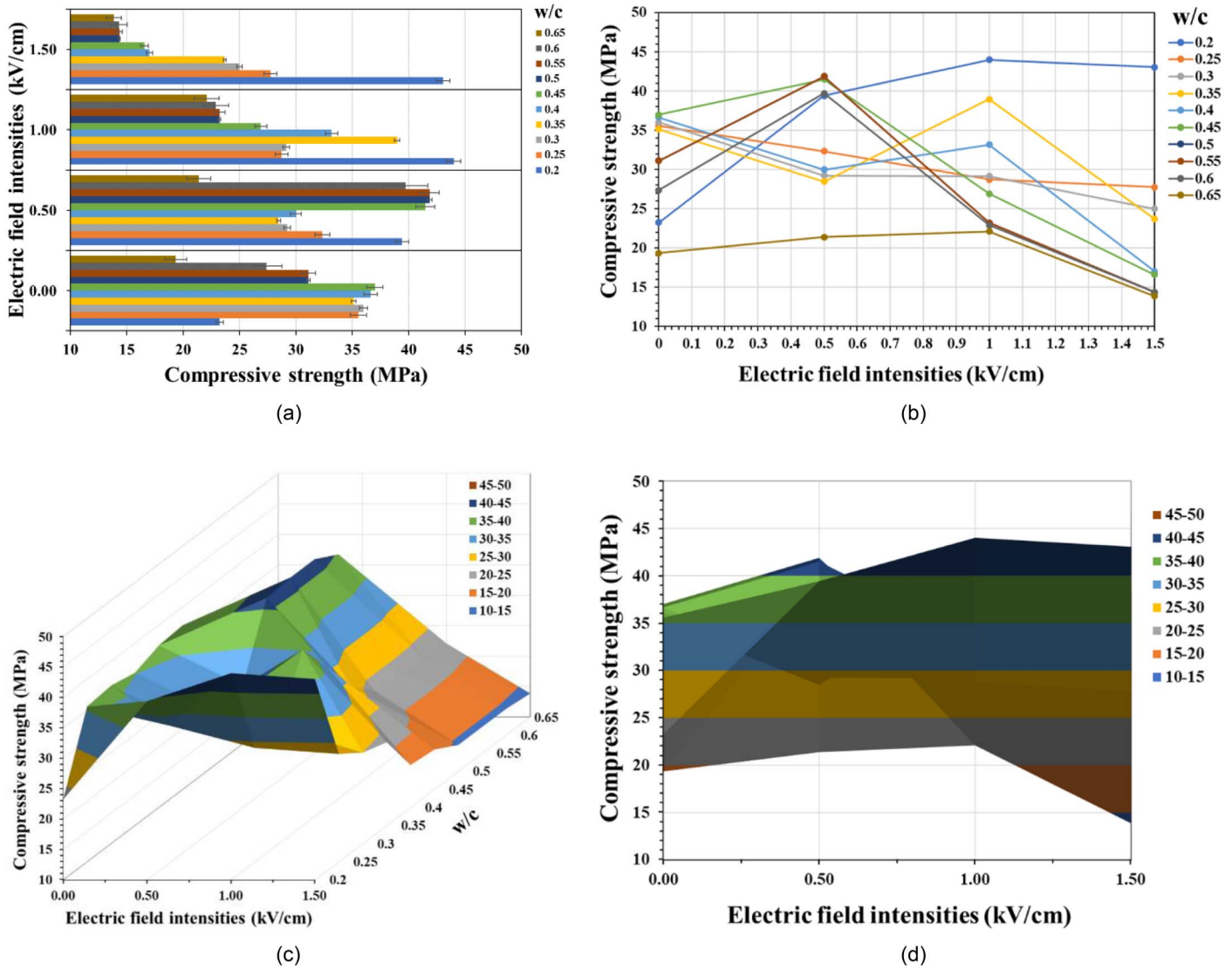

Fig. 6. Compressive strengths of the pastes cured in air (control) and via PEF for 50 min with continuous curing with air for 28 days: (a) compressive strength and electric field intensity, 2D; (b) electric field intensity and compressive strength, 2D; (c) compressive strength, electric field intensity and w/c, 3D; and (d) compressive strength and electric field intensity, 2D.

which alter the pore connectivity unpredictably and weaken the resulting matrix. The net result is that, although these samples show an initial gain in strength, they eventually fall behind the control in their uniformity and final compressive strength.

Another factor involves the relative influence of subsequent air curing. When the PEF treatment ceases, all specimens are placed in ambient conditions (25 ± 2°C) for the remainder of the 28 days. Cracks initiated by thermal or electrochemical phenomena during the first 50 min of PEF can persist unless the hydration process progresses enough to self-heal or fill them with late-forming hydration products. If the w/c ratio is suboptimal, or if the field intensity was high enough to create wide cracks, then air curing might not suffice to heal them. Consequently, those flaws remain embedded in the material, which explains why some PEF-cured specimens in the 0.25–0.40 range fail to match the strengths achieved by the control. Conversely, specimens at 0.45–0.60 under 0.5 kV/cm appear to have enough free water and sufficiently mild field conditions to avoid catastrophic cracking and to benefit from the boosted hydration rate. At 28 days, they exhibit compressive strengths that meet and surpass the highest values achieved for the control, with maximum values of close to 41.0 MPa.

Fig. 6 also shows that it is essential to adjust the electric field intensity to the water content. Although higher electric fields of 1.0 kV/cm and above can dramatically shorten the induction periods and increase the rate of hydration, they can also instigate the formation of microcracking, particularly in dense (low w/c) pastes where heat and reaction byproducts accumulate quickly. These microcracks can be visually observed in some specimens, as per the reference in Figs. 8(a–j) shows the paste specimens cured by air (control, 0.0 kV/cm) and PEF for 50 min (0.5–1.5 kV/cm) and continuous curing with air for 28 days at w/c 0.20–0.65, which depicts apparent fissures and voids. These flaws drastically lower the compressive strength, even if the total amount of C–S–H produced is substantial, because local structural discontinuities reduce the paste's capacity to transfer loads effectively.

In contrast, the data strongly suggest that 0.5 kV/cm is the most favorable compromise for many of the w/c ratios tested here, and especially for values of around 0.45–0.60. This intermediate electric field strength intensity facilitates the robust formation of hydration products early in the curing window, accelerating strength gain without generating severe temperature gradients or extensive electrolysis. When combined with a water content that is sufficient to

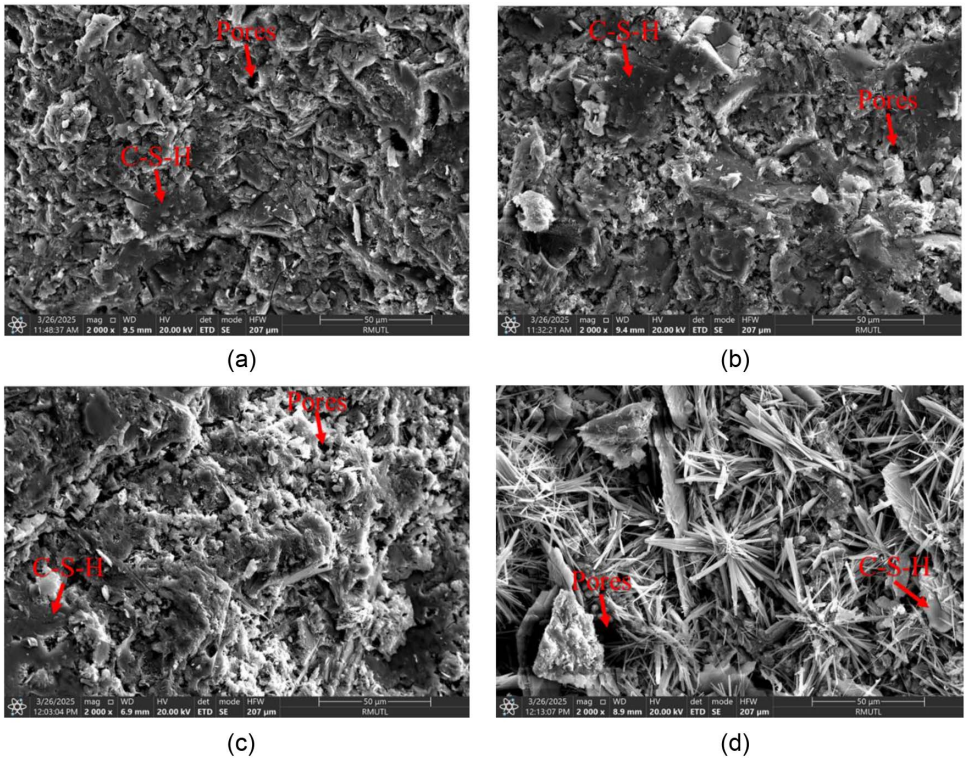

Fig. 7. SEM images showing microstructure and pore percentages (%) for w/c 0.45: (a) control (0.0 kV/cm), 30.247%; (b) 0.5 kV/cm, 28.613%; (c) 1.0 kV/cm, 31.092%; and (d) 1.5 kV/cm, 41.134%.

handle local heat spikes and maintain partial fluidity, the result is a dense, well-hydrated microstructure at the end of 28 days. The control specimens, which lack any electric field assistance, generally show steadier but slower hydration, which can lead to a consistent microstructure without achieving the same early-age performance. Although the control might occasionally match or surpass certain PEF-cured mixtures that suffer from microcracks, it cannot exceed the best-performing PEF condition (i.e., 0.5 kV/cm with a suitably moderate w/c ratio).

One important aspect is that these observations closely map to well-known cement science principles regarding hydration kinetics and porosity. A small or moderate field can act as a mild accelerator, driving ionic species where they are needed without overshooting the thermal or mechanical equilibrium required by the paste. The synergy between a slight electrochemical stimulation and an adequate water supply fosters uniform, crack-free hydration layers. The data show that if this synergy is lost due to excessive field strength or insufficient (or excessive) water content, the final product resembles a typically cured control sample, or exhibits cracks and suboptimal strength. Hence, Fig. 6 clearly demonstrates that it is only when the fundamental reaction parameters (w/c ratio, electric field intensity, and curing regimen) are harmoniously aligned that PEF can truly outperform traditional methods without a reduced final strength.

Fig. 9 shows the relationships between the compressive strength results for cement samples formulated with diverse w/c ratios, from 0.20 to 0.65, under four distinct PEF conditions: (a) no electric field (control); (b) 0.5 kV/cm; (c) 1.0 kV/cm; and (d) 1.5 kV/cm. Analysis of these graphs gives several pivotal insights into how PEF intensity and moisture content influence the late-age mechanical characteristics.

For the control series [Fig. 9(a)], the compressive strength generally reaches a peak in the intermediate range of w/c ratios ($\approx$0.30–0.50) before diminishing as free water becomes excessive (w/c $\geq$ 0.60). This traditional pattern reflects the compromise between the availability of sufficient water to complete hydration and an excess, which results in increased porosity and reduced strength. At 0.5 kV/cm PEF [Fig. 9(b)], it is evident that specific w/c ratios, particularly in the vicinity of 0.45 to 0.60, benefit markedly from the modest acceleration of hydration. The initial ion mobility appears optimized within this range, promoting robust C–S–H networks that translate into elevated 28 day strengths (up to ~41 MPa). Conversely, at very low w/c (e.g., 0.20), the matrix is so dense that even moderate PEF intensities can induce localized heating and internal stress, occasionally resulting in microcracking that may counterbalance the gains from accelerated hydration. However, 0.5 kV/cm gives uniformly superior strengths compared to the control under many of the conditions examined here, indicating an advantageous synergy between gentle electric stimulation and adequate availability of water for the proliferation of hydration products.

The response becomes more polarized when the electric field is increased to 1.0 kV/cm [Fig. 9(c)]. While some mixtures with lower w/c ratios exhibit enhancements over the control, others show underperformance or erratic outcomes, which are likely to be due to overheating or the formation of superficial hydration shells that hinder a deeper reaction (referred to as the "shell effect") (Gurski et al. 2023; Zhou et al. 2023; Marković 1984). Strong PEF conditions can engender microvoids or microcracks in the early curing phases, reducing the ultimate compressive strength. Comparable or even more pronounced challenges arise at 1.5 kV/cm [Fig. 9(d)], as high-intensity pulses can deliver a rapid, near-instantaneous surge of hydration alongside substantial internal stress. Although these pulses can increase the early-age strength, the intense local temperature and pore-fluid pressure may foster cracks, shrinkage stress, or electrolysis bubbles, culminating in compromised, discontinuous

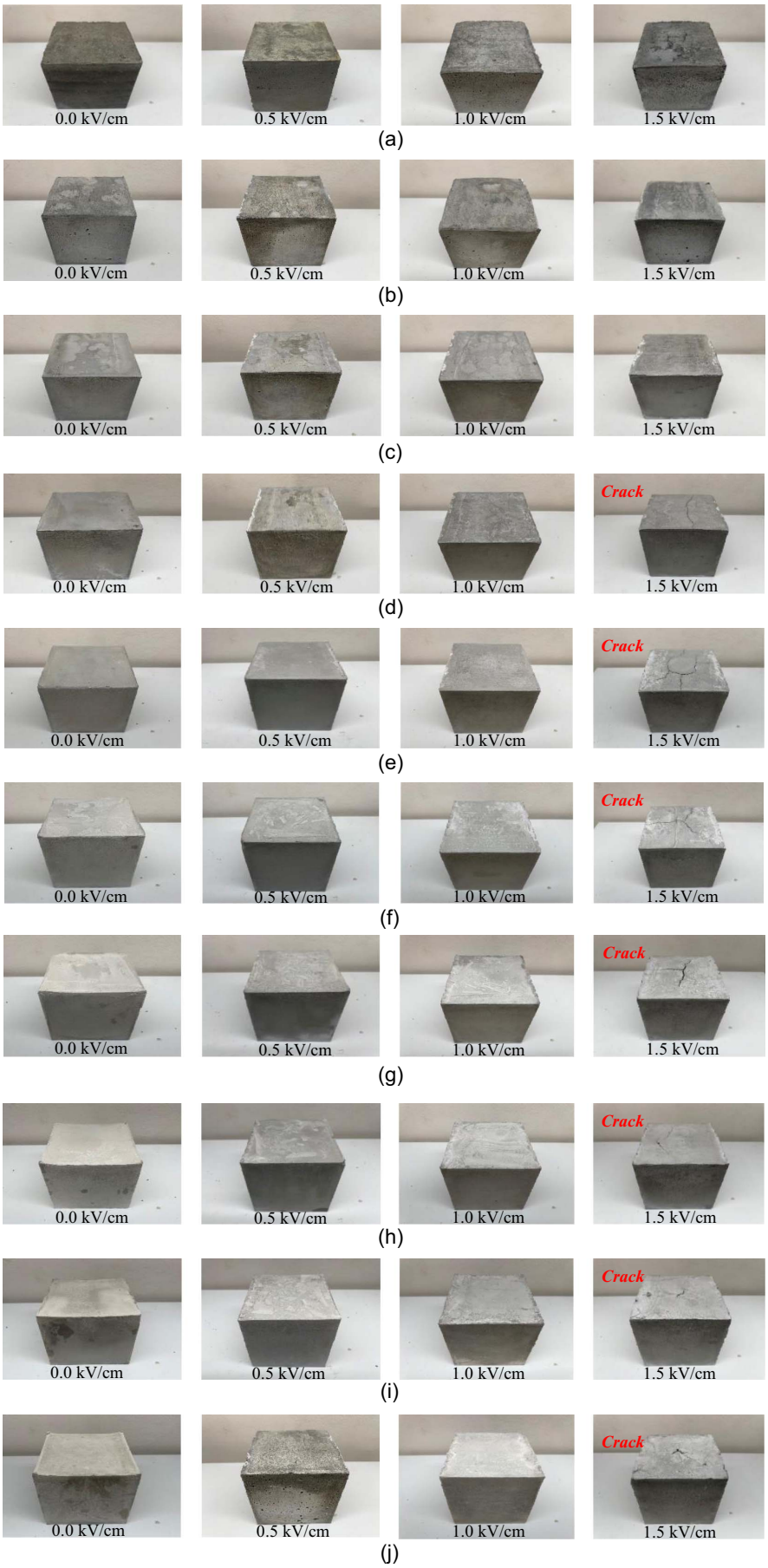

Fig. 8. Paste specimens cured by air (control, 0.0 kV/cm) and PEF for 50 min (0.5–1.5 kV/cm) and continuous curing with air for 28 days: (a) w/c 0.20; (b) w/c 0.25; (c) w/c 0.30; (d) w/c 0.35; (e) w/c 0.40; (f) w/c 0.45; (g) w/c 0.50; (h) w/c 0.55; (i) w/c 0.60; and (j) w/c 0.65.

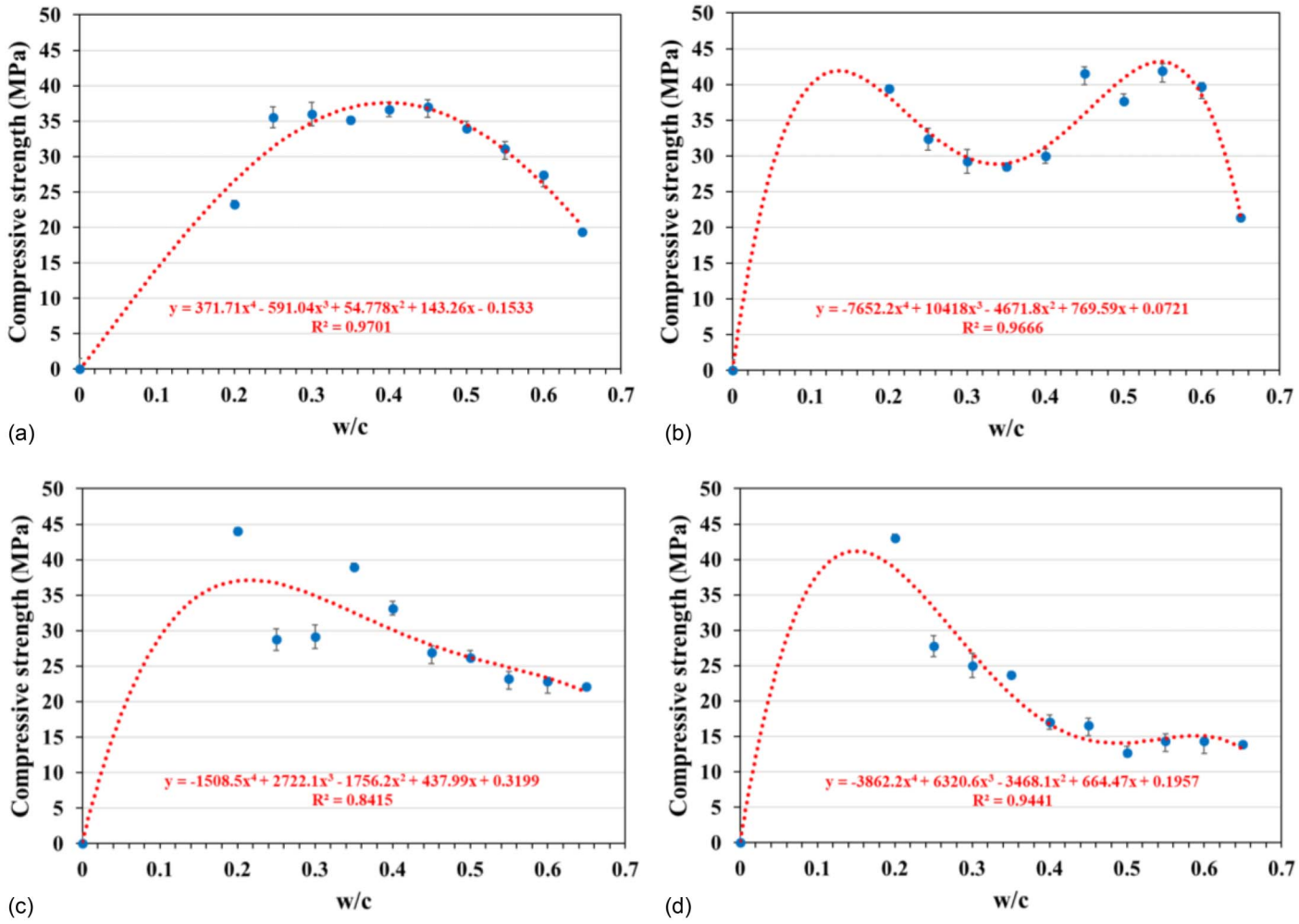

Fig. 9. Relationships between compressive strengths of the pastes and w/c: (a) control (0.0 kV/cm); (b) PEF at 0.5 kV/cm; (c) PEF at 1.0 kV/cm; and (d) PEF at 1.5 kV/cm.

microstructures by day 28. In several instances, 1.5 kV/cm yields strengths that do not exceed, or even match, those attained at 0.5 kV/cm.

This section focuses on characterizing the primary hydration products in cement pastes, CH, and C–S–H, via XRD, as shown in Fig. 10. Cement hydration is driven by the reactions between water and the major clinker phases (e.g., C_3S and C_2S), producing a multiphase microstructure whose crystalline and semicrystalline components largely govern the mechanical and durability properties. Of these reaction products, calcium hydroxide ($Ca(OH)_2$) often appears as well-defined crystalline peaks in XRD due to its relatively organized crystal lattice. C–S–H is typically identified indirectly, as it predominantly exists in an amorphous or poorly crystalline state. An evaluation of the intensity and position of CH reflections can provide insights into the overall degree of cement hydration, since CH readily precipitates once tricalcium silicate begins to dissolve. Concurrently, broad humps in the XRD profile (often in the 25°–35° 2θ range) can denote C–S–H gel, reflecting its inherently disordered structure (Mesecke et al. 2022).

In practical terms, XRD analysis of hydrated cement pastes often reveals that moderate concentrations of $Ca(OH)_2$ emerge at early ages and grow more pronounced with ongoing hydration, whereas the "halo" indicative of C–S–H tends to broaden over time. The formation of CH peaks and enhanced amorphous humps for C–S–H are intensified if curing processes such as PEF treatment are used to accelerate the dissolution of clinker phases. Evidence of higher CH peak intensities in the PEF-cured specimens suggests that the early hydration processes (particularly of tricalcium silicate) have been expedited, releasing more Ca^{2+} and OH^- into a solution for rep-recipitation. Meanwhile, the incipient presence of unreacted clinker peaks (such as alite or belite) may be comparatively subdued at certain ages if PEF has significantly shortened the induction period.

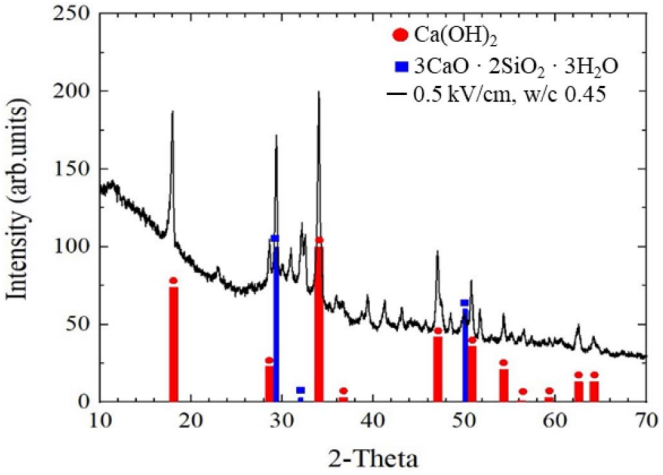

Fig. 10. XRD results, calcium hydroxide [$Ca(OH)_2$] and C–S–H).

Likewise, any shifting of characteristic CH reflections (for instance, near values for 2θ of 18°, 34°, and 47°) might reflect microstructural stress or lattice distortion imparted during the rapid formation of hydration products. Assessments of these XRD signatures for CH and C–S–H under varying PEF intensities and w/c ratios can thus provide a clearer picture of the interplay between accelerated ion transport and the kinetics of phase evolution as well as demonstrate how carefully calibrated electric fields can refine (or, if overly aggressive, disrupt) the hydration matrix.

Discussion

Cement hydration is governed by the interactions among key clinker phases (e.g., C_3S, C_2S, C_3A) and water, culminating in the precipitation of C–S–H, CH, and other minor constituents that together form the load-bearing microstructure. Under conventional, diffusion-controlled curing processes, ions such as Ca^{2+} and OH^- migrate at rates that are determined mainly by concentration gradients, with the dissolution–precipitation sequence unfolding at a pace constrained by the temperature, the availability of water, and the intrinsic reaction kinetics. The Nernst–Planck equation offers a concise framework for capturing this ionic flux, J_i, where the total movement of each Species *iii* (e.g., Ca^{2+} and OH^-) is the sum of a diffusion component (proportional to ∇c_i) and a migration component (proportional to E, the electric field). In a standard setting, diffusion dominates, meaning that concentration gradients drive the dissolution of cement phases and the formation of hydration products relatively slowly. When PEF is introduced, however, the additional electromigration term, $z_i F \mu_i c_i E$, can vastly surpass normal diffusion, effectively stimulating faster ion transport for reaction with partially dissolved cement grains (Huang et al. 2023c; Rolle et al. 2018). This acceleration shortens the induction period of hydration, during which dissolution initially lags, thereby advancing the formation of C-S-H, CH, and other hydrates. However, although the Nernst–Planck equation captures the enhanced ionic flux, it gives little information about the subsequent exothermic heat release from cement hydration. Local temperature rises are a direct byproduct of accelerating this dissolution–precipitation reactions: these can be beneficial if carefully managed, as they improve the early-age strength, but may be detrimental if they spawn thermal cracks or microstructural "shells." Another central factor is the w/c ratio, which governs the paste's porosity and capacity to dissipate heat. Low w/c mixtures develop higher strengths under normal conditions but present fewer pathways for heat and mass transfer, making them more susceptible to thermal or stress-induced defects under strong electric fields. Conversely, higher w/c mixtures can absorb more significant thermal spikes at the cost of an inherently weaker ultimate microstructure. An understanding of the synergy among Nernst–Planck transport, hydration kinetics, and w/c ratio is thus essential in terms of reaping the maximum benefits of PEF curing while minimizing undesirable effects such as microcracking, excessive porosity, or incomplete hydration of grains (Huang et al. 2023a, b, c).

On a fundamental level, the hydration kinetics of cement revolve around the dissolution of tricalcium silicate (C_3S) and dicalcium silicate (C_2S) in water, generating ionic species that reassemble into C–S–H, the primary strength-giving phase. This process is exothermic, and the local release of heat can further expedite chemical reactions, yielding a positive feedback loop for early-age strength development. However, without an external field, ion transport is comparatively slow, regulated by diffusion through water-filled pores, and augmented only slightly by increases in temperature. The introduction of PEF significantly modifies these conditions. During each pulse, cationic species (Ca^{2+} and OH^-) are actively driven through the pore network, promoting quicker contact with unhydrated cement surfaces and thus triggering a steeper chemical gradient. This phenomenon reduces the induction period and can also concentrate reactants in certain regions. The w/c ratio is an important moderator of this effect: at low w/c (e.g., 0.20–0.30), the matrix is dense, so although the electric field can accelerate hydration, the narrow pore structure traps heat and reaction byproducts. If the field intensity is too high, localized temperature surges exceeding 80°C or more generate microcracking and hinder long-term durability (Yousuf and Xiaosheng 2021; Zheng et al. 2021; Huang et al. 2023c). At moderate to high values of w/c (≈0.45–0.60), the additional free water confers excellent thermal and ionic buffering capacity, making the cement paste more forgiving under accelerated curing, although the trade-off is an inherent decline in ultimate strength due to increased porosity. Striking a balance often gives an optimal w/c window of around 0.40–0.50, whereby the electric field can boost early hydration without imposing excessive thermal stress or leaving behind large, interconnected pores. Under these conditions, Nernst–Planck-driven migration fosters homogenous propagation of the hydration front, leading to denser distribution of the C–S–H gel across the matrix. In effect, the synergy between moderate w/c ratios and suitably tuned electric field intensities (often around 0.5 kV/cm) can outperform both purely diffusive curing (where the reaction is limited by slow ion transport) and high-field curing in dense pastes.

An essential effect of rapid hydration is the thermal rise at early ages, which stems directly from exothermic reactions. In instances where the PEF intensity is 1.0 kV/cm or higher, low w/c pastes (e.g., 0.20–0.25) frequently undergo abrupt thermal gradients, which may reach 85°C–90°C within a few hours. These temperatures significantly transcend conventional steam-curing levels for standard structural concretes and can induce microfissures or partial "shell" formation, a phenomenon wherein the excessively rapid precipitation of hydrates near the external surfaces of cement grains prevents water and ions from reaching the grain interiors. Conversely, if the w/c ratio is high (≥0.60), the thermal spike may be diminished, but the porosity is increased, thereby capping the ultimate strength.

Electrolysis under potent fields in high-w/c mixtures can also generate gas bubbles that degrade the microstructure. Consequently, the PEF curing process requires meticulous calibration of the availability of water, field intensity, and pulse characteristics (duration, frequency) to regulate exothermic acceleration and potential microstructural disruption (Huang et al. 2023b; Aitcin and Neville 2003). Electroosmotic flow is another relevant effect: pulsed fields can mobilize water molecules within the paste, a process that is beneficial if it reaches zones that are susceptible to desiccation but detrimental if it engenders a moisture imbalance, as it leads to localized hot spots. Upon cessation of the electric pulses, the system typically transitions to a conventional curing environment at approximately 25°C. Any fissures instigated by the thermal surge may self-repair if the fissures are minor and free water persists. However, substantial defects may endure, meaning that the final strength is reduced despite the plentiful net content of hydration products. This interplay among electric field parameters, w/c ratio, and subsequent ambient curing dictates the final distribution of pores, fissures, and unhydrated clinker grains and can profoundly influence the compressive strength at 28 days and beyond. Empirical evidence shows that 0.5 kV/cm is often a nearly optimal compromise for numerous mixture designs, as it provides sufficient impetus to truncate the induction phases without eliciting the extreme thermal or electrochemical byproducts that impede performance. However, the precise synergy relies on the intricate details of the cement composition, mixing methodology, electrode configuration, and pulse scheduling.

The unification of the Nernst–Planck equation, hydration kinetics, and assorted w/c ratios clarifies the framework within which PEF can substantially accelerate the curing of cement paste. The Nernst–Planck paradigm illustrates how electromigration can significantly expedite ion transport beyond diffusion-restricted velocities, facilitating rapid dissolution of clinker minerals and swift precipitation of C–S–H. However, this increase in the reaction rate means that meticulous regulation is needed via the w/c ratio to equilibrate heat dispersion and water accessibility. An excessively low w/c engenders a dense matrix that is vulnerable to microcracking under elevated electric fields, whereas an excessively high w/c produces an overly porous framework that limits the ultimate strength. Under ideal conditions, moderate w/c pastes (~0.40–0.50) exposed to fields approximately 0.5–1.0 kV/cm can achieve a productive equilibrium, with a considerable reduction in the curing duration and enhanced early-age strength, culminating in a resilient final microstructure with minimized pore size and distribution. Future work should focus on refining computational models that integrate Nernst–Planck ion transport with the thermal and mechanical stresses arising from hydration, to enable practitioners to align field intensities with specific mix formulations more accurately. Such instruments may incorporate real-time feedback from embedded sensors to modulate pulse sequences or intensities in situ to preclude microstructural compromise. Further, the substitution of partial quantities of cement with supplementary materials such as fly ash or slag would introduce additional chemical interactions that could modify the hydration rate, further complicating the synergy with PEF. These burgeoning avenues of research attest to the potential of PEF in terms of promoting sustainable, high-performance concrete construction. By transcending the conventional diffusion-limited hydration paradigm, engineers can realize rapid early strength advancements while reducing the total energy expenditure in comparison to traditional steam curing. When properly used, PEF acceleration can be integrated with contemporary approaches to construction to offer speed, efficacy, and durability, although scientifically grounded calibration of each parameter (electric field amplitude, w/c ratio, mixing design, and curing schedule) is important in order to extract maximum benefit from the phenomenon of Nernst–Planck-driven acceleration (Saxena et al. 2024; Li et al. 2022).

Conclusion

This study has examined the accelerated curing of cement pastes by PEF, with a focus on the influence of water content on hydration and microstructural development. Key findings and conclusions include the following:

- An electric field intensity of 0.5 kV/cm with w/c ratios of 0.40–0.45 significantly accelerated early hydration and improved the 28 day strength by up to 20%.
- An excessive electric field intensity (>1.0 kV/cm) caused microcracking in low w/c mixtures due to thermal stress and rapid reactions.
- The water content influenced the ion transport and heat dissipation, with low and high w/c ratios posing risks under strong fields.
- PEF curing shortened the curing time and reduced energy use, although temperature control is essential to avoid damage.
- Optimization of the PEF parameters offers a promising path for striking a balance between early strength and long-term durability, with potential for scale-up and integration with sustainable materials.
- This study proposes a novel nonthermal approach to accelerating cement curing using PEF and highlights the significant influence of water content on electrothermal responses, an aspect that has not been clearly addressed in prior research.

Data Availability Statement

Some or all data, models, or code that support the findings of this study are available from the corresponding author upon reasonable request.

Acknowledgments

This project was funded by the National Research Council of Thailand (NRCT; Contract No. N42A660953), and the research was supported by the Thailand Science Research and Innovation (TSRI) Fundamental Fund in fiscal year 2024 and 2025. We also acknowledge the support Hub of Talents Electromagnetic Energy Utilization in Medical Engineering (TEEUME), Department of Mechanical Engineering, Faculty of Engineering, Thammasat University, and Material Science Center, Faculty of Industrial Technology, Phanakhon Rajabhat University, and Research Unit of Applied Electric Field in Engineering (RUEE), College of Integrated Science and Technology Rajamangala University of Technology Lanna during the project.

Author Contributions

Chatchawan Kantala: Conceptualization; Data curation; Formal analysis; Funding acquisition; Investigation; Methodology; Project administration; Resources; Software; Supervision; Validation; Visualization; Writing – original draft; Writing – review and editing. Natt Makul: Methodology; Project administration; Supervision. Phadungsak Rattanadecho: Conceptualization; Formal analysis; Methodology; Supervision; Writing – review and editing.

References

Aitcin, P. C., and A. Neville. 2003. "How the water-cement ratio affects concrete strength." *Concr. Int.* 25 (8): 51–58.

ASTM. 2017. *Standard performance specification for hydraulic cement*. ASTM 91.100.10. West Conshohocken, PA: ASTM.

Bredenkamp, S., K. Kruger, and G. L. Bredenkamp. 1993. "Direct electric curing of concrete." *Mag. Concr. Res.* 45 (Mar): 71–74. https://doi.org/10.1680/macr.1993.45.162.71.

BSI (British Standards Institution). 1983. *Testing concrete—Part 3: Method for making and curing test specimens for strength tests*. BS 1881-3. London: BSI.

Che, J., J. Gu, S. Zhao, C. Liu, H. Liu, and S. C. Chin. 2025. "Study on the influence of supplementary cementitious materials on fast hardening sulfoaluminate cement–engineered cementitious composites." *J. Mater. Civ. Eng.* 37 (6): 19226. https://doi.org/10.1061/JMCEE7.MTENG-19336.

Engel'sht, V. S., and V. Z. Muratalieva. 2013. "The exothermal effect upon interaction of calcium and silicon oxides." *High Temp.* 51 (5): 645–651. https://doi.org/10.1134/S0018151X13040068.

Gawel, K., S. Wenner, N. Jafariesfad, M. Torsæter, and H. Justnes. 2022. "Portland cement hydration in the vicinity of electrically polarized conductive surfaces." *Cem. Concr. Compos.* 134 (Nov): 104792. https://doi.org/10.1016/j.cemconcomp.2022.104792.

Gurski, G. S., H. Kirchberg, P. Nalbach, and M. Thorwart. 2023. "Hydration shell effects in ac-driven single-molecule junctions." *Phys. Rev. B* 107 (16): 165413. https://doi.org/10.1103/PhysRevB.107.165413.

Hao, H., I. Leven, and T. Head-Gordon. 2022. "Can electric fields drive chemistry for an aqueous microdroplet?" *Nat. Commun.* 13 (1): 280. https://doi.org/10.1038/s41467-021-27941-x.

He, Z., H. Cui, S. Hao, L. Wang, and J. Zhou. 2018. "Electric-field effects on ionic hydration: A molecular dynamics study." *J. Phys. Chem. Lett.* 122 (22): 5991–5998. https://doi.org/10.1021/acs.jpcb.8b02773.

Horne, F. H. 1983. "Application of irreversible thermodynamics to mass transport in ionic conductors." In *The physics of superionic conductors and electrode materials*, edited by J. W. Perram. Boston: Springer. https://doi.org/10.1007/978-1-4684-4490-2_15.

Huang, F. H., Z. Hu, S. Li, J. Liu, F. Y. Han, and J. Liu. 2023a. "Long-term deformation and mechanical properties evolution of cement paste with ultra-low water-to-cement ratio driven by water migration." *J. Build. Eng.* 76 (Oct): 107250. https://doi.org/10.1016/j.jobe.2023.107250.

Huang, H., S. Zhang, Y. Wang, Y. Guo, C. Zhang, and F. Qu. 2025. "Cement-based electrochemical systems for structural energy storage: Progress and prospects." *Materials* 18 (15): 3601. https://doi.org/10.3390/ma18153601.

Huang, P. W., B. Flemisch, C. Qin, M. O. Saar, and A. Ebigbo. 2023b. "Validating the Nernst–Planck transport model under reaction-driven flow conditions using RetroPy v1.0." *Geosci. Model Dev.* 16 (16): 4767–4791. https://doi.org/10.5194/gmd-16-4767-2023.

Huang, Q., H. Liu, Q. Wang, Y. Shan, D. Tang, Z. Zhang, and X. Zhu. 2023c. "Electric field-induced deterioration of cement mortars owing to calcium leaching." *Dev. Built Environ.* 17 (Mar): 100303. https://doi.org/10.1016/j.dibe.2023.100303.

Kuznetsova, N., V. Lopatin, V. Burkin, V. Golovanevskiy, D. Zhgun, and N. Ivanov. 2011. "Theoretical and experimental investigation of electro discharge destruction of non-conducting materials." In *Proc. IEEE Int. Pulsed Power Conf.*, 267–273. New York: IEEE. https://doi.org/10.1109/PPC.2011.6191428.

Lee, S. I., C. U. Kim, and C. H. Lee. 2023. "Optimum curing regimes of early strength concrete inclusive of heat transfer and hydration effects." *J. Mater. Civ. Eng.* 35 (7): 15077. https://doi.org/10.1061/JMCEE7.MTENG-15077.

Li, G., C. Zhou, W. Ahmad, K. I. Usanova, M. Karelina, A. M. Mohamed, and R. Khallaf. 2022. "Fly ash application as supplementary cementitious material: A review." *Materials* 15 (7): 2664. https://doi.org/10.3390/ma15072664.

Li, M., W. Sun, H. Wang, and M. Li. 2023. "Multiphysics effect study of high-voltage electrical pulses on rock pores." In *Proc., 2023 IEEE 3rd Int. Conf. on Electronic Technology, Communication and Information*, 1063–1067. New York: IEEE. https://doi.org/10.1109/ICETCI57876.2023.10176894.

Li, X., J. Wang, S. Li, X. Gao, and Z. Shi. 2025. "Application of low-temperature microwave radiation on the preparation of UHPC." *Low-Carbon Mater. Green Constr.* 3 (1): 3. https://doi.org/10.1007/s44242-025-00063-z.

Liu, H., N. Shi, K. S. Han, X. Fu, and F. Yu. 2024. "Study on the attack of concrete by external sulfate under electric fields." *Coatings* 14 (8): 1008. https://doi.org/10.3390/coatings14081008.

Lyutikova, M. N., S. M. Korobeinikov, and V. V. Buzaev. 2020. "Determination of water content in liquid insulation of high-voltage equipment by different methods." *Power Technol. Eng.* 53 (5): 623–630. https://doi.org/10.1007/s10749-020-01127-9.

Ma, C., F. Dai, J. Shi, D. Song, B. Dong, H. Zhou, and Y. B. Du. 2023. "Achieving energy savings and early-ages strength enhancement of prefabricated cement components: Combined application of direct electric curing and sodium sulphate." *J. Cleaner Prod.* 425 (Nov): 138802. https://doi.org/10.1016/j.jclepro.2023.138802.

Ma, C., J. Peng, H. Zhou, Z. Rui, W. Ren, and Y. Du. 2021. "An effective method for preparing high early-strength cement-based materials: The effects of direct electric curing on portland cement." *J. Build. Eng.* 43 (Nov): 102485. https://doi.org/10.1016/j.jobe.2021.102485.

Makul, N., and G. Sua-iam. 2024. "New insights into early-stage time-dependent dielectric characteristics coupled with frequency dependency and hydration-driven reaction of hydraulic cement pastes: Experiments and statistical modelling." *J. Build. Eng.* 88 (Jul): 109118. https://doi.org/10.1016/j.jobe.2024.109118.

Mangat, P. S., S. Abubakri, K. Grigoriadis, and V. Starinieri. 2021. "Hydration and microwave curing temperature interactions of repair mortars." *Prog. Mater. Sci.* 3 (4): 040. https://doi.org/10.21926/rpm.2104040.

Marković, Z. 1984. "Electric polarization of w/o-microemulsions: Studies using electric birefringence." In *Reverse micelles. Forschung Soziologie*, edited by P. L. Luisi and B. E. Straub. Boston: Springer. https://doi.org/10.1007/978-1-4757-6424-6_19.

Mengistu, A. G., L. D. van Rensburg, and S. S. W. Mavimbela. 2017. "The effect of soil water and temperature on thermal properties of two soils developed from aeolian sands in South Africa." *Catena* 158 (Nov): 184–193. https://doi.org/10.1016/j.catena.2017.07.001.

Mesecke, K., L. N. Warr, and W. Malornya. 2022. "Structure modeling and quantitative X-ray diffraction of C-(A)-S-H." *J. Appl. Cryst.* 55 (1): 133–143. https://doi.org/10.1107/S1600576721012668.

Nepomnyashchev, G. A., and M. M. Titov. 2023. "Increasing cement strength properties with electrophysical processing of water-cement suspension." *Вестник Томского Государственного Архитектурно-Строительного Университета* 25 (4): 161–175. https://doi.org/10.31675/1607-1859-2023-25-4-161-175.

Osuna, R. I. A., P. Cobelli, and N. M. Olaiz. 2022. "Bubble formation in pulsed electric field technology may pose limitations." *Micromachines* 13 (8): 1234. https://doi.org/10.3390/mi13081234.

Qi, C., X. Xu, and Q. Chen. 2021. "Hydration reactivity difference between dicalcium silicate and tricalcium silicate revealed from structural and Bader charge analysis." *Int. J. Miner. Metall. Mater.* 29 (2): 335–344. https://doi.org/10.1007/s12613-021-2364-5.

Rolle, M., R. Sprocati, M. Masi, B. Jin, and M. Muniruzzaman. 2018. "Nernst–Planck based description of transport, coulombic interactions and geochemical reactions in porous media: Modeling approach and benchmark experiments." *Water Resour. Res.* 54 (4): 3176–3195. https://doi.org/10.1002/2017WR022344.

Sánchez, E. M., J. P. Piñón, A. M. Ramírez, J. M. Lopez-Romero, M. G. Martinez, and G. O. S. Vega. 2024. "Method for measuring the setting process of cement-water mixtures by electrical impedance." *Superficies y Vacío* 37: 240101. https://doi.org/10.47566/2024_syv37_1-240101.

Saxena, H. M., V. Srivastava, A. K. Yadav, and A. K. Tiwari. 2024. "Ultrafine GGBS and fly ash as cement replacement for sustainable concrete." *J. Environ. Nanotechnol.* 13 (3): 25–30. https://doi.org/10.13074/jent.2024.09.242659.

Schottroff, F., J. Knappert, P. Eppmann, A. Krottenthaler, T. Horneber, C. McHardy, C. Rauh, and H. Jaeger. 2020. "Development of a continuous PEF vortex-flow chamber for improved treatment homogeneity based on hydrodynamic optimization." *Front. Bioeng. Biotechnol.* 8 (Apr): 340. https://doi.org/10.3389/fbioe.2020.00340.

Smith, S., S. Griffiths, S. MacGregor, J. Beveridge, J. Anderson, C. Walle, and M. H. Grant. 2009. "Pulsed electric field as a potential new method for microbial inactivation in scaffold materials for tissue engineering: The effect on collagen as a scaffold." *J. Biomed. Mater. Res. A.* 90 (3): 844–851. https://doi.org/10.1002/jbm.a.32150.

Susanto, A., D. A. Koleva, E. A. B. Koenders, and K. V. Breugel. 2015. "A conceptual model for ionic transport in cement-based materials in conditions of externally applied electric field." *MRS Proc.* 1768 (Jan): 49–55. https://doi.org/10.1557/opl.2015.325.

Wang, J., S. Liu, Y. Cai, X. Ren, Y. Xiang, K. Yang, Y. Li, Z. Tang, and G. Long. 2023. "Effect of precuring time on the strength, microstructure, and energy consumption of direct electric curing concrete." *J. Build. Eng.* 80 (2): 107963. https://doi.org/10.1016/j.jobe.2023.107963.

Wu, S. 2023. "Investigations of the optimal requirements for curing of calcium sulfoaluminate cement systems." *Cement* 12 (Jun): 100072. https://doi.org/10.1016/j.cement.2023.100072.

Yang, P., G. Sant, and N. Neithalath. 2017. "A refined, self-consistent Poisson–Nernst–Planck (PNP) model for electrically induced transport of multiple ionic species though concrete." *Cem. Concr. Compos.* 82 (Sep): 80–94. https://doi.org/10.1016/j.cemconcomp.2017.05.015.

Yang, Z., Y. Xie, J. He, F. Wang, X. Zeng, K. Ma, and G. Long. 2021. "Comparative study on the mechanical properties and microstructure of cement-based materials by direct electric curing and steam curing." *Materials* 14 (23): 7407. https://doi.org/10.3390/ma14237407.

Yousuf, F., and W. Xiaosheng. 2021. "Water to cement ratio effect on cement paste microstructural development by electrical resistivity measurements and computer illustration." *Am. J. Civ. Eng. Archit.* 9 (3): 73–87. https://doi.org/10.12691/AJCEA-9-3-1.

Zhang, G., K. Li, L. Like, S. Huawei, C. Chen, and C. Yuan. 2024. "Influence mechanism of accelerator on the hydration and microstructural properties of portland cement." *Buildings* 14 (10): 3201. https://doi.org/10.3390/buildings14103201.

Zheng, W., J. Dong, J. Wen, C. Chenggong, and X. Xueying. 2021. "Effects of water-to-cement ratios on the properties of magnesium potassium phosphate cement prepared with lithium-extracted magnesium residue." *Appl. Sci.* 11 (9): 4193. https://doi.org/10.3390/app11094193.

Zhou, W., Y. Guo, Z. Zhang, W. Guo, and H. Qiu. 2023. "Field-induced hydration shell reorganization enables electro-osmotic flow in nanochannels." *Phys. Rev. Lett.* 130 (8): 084001. https://doi.org/10.1103/PhysRevLett.130.084001.